weight) previously obtained by purification (*5*). Therefore, the inhibition of GTP cyclohydrolase I in rat liver appears to be fully dependent on the concentrations of p35, BH_4, and GTP. Dependence on the concentration of GTP cyclohydrolase I itself was also observed when the p35 concentration in the reaction mixture was reduced to one-fifth of its physiological concentration, and the EC_{50} of GTP cyclohydrolase I was 0.8 nM under such conditions.

15. This effect was highly specific to L-phenylalanine, and the following compounds were totally ineffective at a concentration of 1 mM: D-phenylalanine, β-phenylpyruvic acid, and phenethylamine (the immediate degradation products of phenylalanine), L-tryptophan and L-tyrosine (the substrates of tryptophan and tyrosine hydroxylase, respectively), and L-arginine (the substrate of nitric oxide synthases).
16. O. Greengard and J. A. Delvalle, *Biochem. J.* **154**, 619 (1976).
17. The 100,000*g* supernatant of rat liver homogenates was incubated in buffer A [50 mM tris (pH 7.5), 100 mM KCl, and 1 mM EDTA, 1 mM dithiothreitol] containing GTP and BH_4 under conditions that completely inhibited GTP cyclohydrolase I activity. Then the mixture was filtered through Superdex 200pg gel in the equilibration buffers of various compositions. The eluates were collected into four fractions (Fig. 1), and each fraction was concentrated and filtered through a Sephadex G-25 column equilibrated with buffer A. Then each fraction was used for the assay of GTP cyclohydrolase I activity in the presence or absence of BH_4.
18. In immunoprecipitation experiments, similar results were obtained regarding the requirements for complex formation. Using a polyclonal antibody for the NH_2-terminal peptide nine amino acid residues of GTP cyclohydrolase I, we coprecipitated the p35 inhibitory and stimulatory activities with GTP cyclohydrolase I activity in the presence of both BH_4 and GTP or in the presence of phenylalanine. Thus, these experiments, in addition to the gel-filtration experiments, further confirmed the specific interaction of p35 with GTP cyclohydrolase I.
19. S. Milstien and S. Kaufman, *J. Biol. Chem.* **250**, 4777 (1975); M. A. Parniak and J. Pilkington, *Biochem. Cell Biol.* **67**, 293 (1989).
20. S. Kaufman, *Biochem. Soc. Trans.* **13**, 433 (1985).
21. Because the reported apparent Michaelis constants of phenylalanine hydroxylase for BH_4 are in the range of 2 to 15 μM [S. Kaufman and D. B. Fisher, in *Molecular Mechanisms of Oxygen Activation*, O. Hayaishi, Ed. (Academic Press, New York, 1974), pp. 285–369; R. Shiman, *Methods Enzymol.* **142**, 17 (1987)] and the intracellular BH_4 concentration in the liver is about 6 to 8 μM (*13*), this cofactor has been suggested to be one of the rate-limiting factors for phenylalanine hydroxylase. Moreover, we calculated the hepatic concentration of phenylalanine hydroxylase as 6.8 μM, using the reported values for the enzyme's specific activity in crude extracts and as a purified preparation as well as its reported subunit molecular weight [R. Shiman, D. W. Gray, A. Pater, *J. Biol. Chem.* **254**, 11300 (1979)]. This concentration is, surprisingly, nearly equal to that of BH_4, and therefore the hepatic BH_4 content is just enough for one-to-one binding to phenylalanine hydroxylase. In support of this hypothesis, it has been demonstrated that BH_4 restricts the conversion of phenylalanine to tyrosine in the hepatocytes (*19*).
22. C. R. Scriver, S. Kaufman, S. L. C. Woo, in *The Metabolic Basis of Inherited Disease*, C. R. Scriver, A. L. Beaudet, W. S. Sly, D. Valle, Eds. (McGraw-Hill, New York, ed. 6, 1989), pp. 495–546.
23. R. J. Leeming, J. A. Blair, A. Green, D. N. Raine, *Arch. Dis. Child.* **51**, 771 (1976).
24. S. Kaufman *et al.*, *N. Engl. J. Med.* **299**, 673 (1978).
25. R. R. McInnes *et al.*, *J. Clin. Invest.* **73**, 458 (1984).
26. J. L. Dhondt, B. Leroux, J. P. Farriaux, C. Largilliere, R. J. Leeming, *Eur. J. Pediatr.* **141**, 92 (1983).
27. E. R. Stadtman, in *The Enzymes*, student edition, P. D. Boyer, Ed. (Academic Press, New York, 1970), vol. 1, pp. 397–459.
28. Rat liver was homogenized as described (*5*). The supernatant was separated from the residue by centrifugation at 100,000*g* for 30 min and was concentrated twofold by Amicon Centriflo CF25 ultrafiltration. An aliquot (2.5 ml) was applied to a Superdex 200pg column (1.6 cm by 60 cm) (Pharmacia) and eluted with 50 mM tris (pH 7.5), 100 mM KCl, and 1 mM EDTA at 1.0 ml/min. Eluates were monitored for absorbance at 280 nm. Fractions of 1.5 ml were collected, 45 μl of which was assayed for GTP cyclohydrolase I activity and for inhibitory activity in the presence of recombinant GTP cyclohydrolase I (0.1 μg) (*29*).
29. The activity of GTP cyclohydrolase I was assayed as described (*5*). The standard reaction mixture (50 μl) contained 50 mM tris (pH 7.6), 100 mM KCl, 1 mM EDTA, 1 mM dithiothreitol, 0.1 mM GTP, and the enzyme. The reaction was carried out at 37°C for 15 min. Then the reaction product, dihydroneopterin triphosphate, was converted to neopterin by oxidation with I_2 and KI, and dephosphorylation by alkaline phosphatase was performed as described (*5*). Finally, neopterin was quantitated by high-performance liquid chromatography and fluorescent detection.
30. We thank K. Takai, O. Takikawa, and D. Yamamoto for advice; T. Maeda and H. Mori for human liver tissue; Y. Umeda for ion-spray mass spectrometric analysis; and M. Kawaichi, K. Shirabe, and T. Yano for comments on the manuscript. This study was supported by a grant-in-aid for scientific research from the Ministry of Education, Science, and Culture of Japan (K.H.).

30 November 1992; accepted 16 April 1993

Antisense Gene Inhibition by Oligonucleotides Containing C-5 Propyne Pyrimidines

Richard W. Wagner,* Mark D. Matteucci, Jason G. Lewis, Arnold J. Gutierrez, Courtney Moulds, Brian C. Froehler*

Phosphorothioate oligodeoxynucleotides containing the C-5 propyne analogs of uridine and cytidine bind RNA with high affinity and are potent antisense inhibitors of gene expression. In a cellular assay, gene-specific antisense inhibition occurred at nanomolar concentrations of oligonucleotide, was dose-dependent and exquisitely sensitive to sequence mismatches, and was correlated with the melting temperature and length of oligonucleotide. Activity was independent of RNA target site and cell type but was detectable only when the oligonucleotides were microinjected or delivered with cell-permeabilizing agents. These oligonucleotides may have important applications in therapy and in studies of gene function.

Oligodeoxynucleotides (ODNs) offer great promise as antisense agents for the sequence-specific inhibition of gene expression (*1*). Previously, high concentrations of ODNs have been required to elicit biological effects, frequently leading to nonspecific inhibition of gene expression (*2*, *3*). There has rarely been a direct demonstration of ODNs entering cells and blocking protein expression through sequence-specific RNA interactions. In general, the deficiencies of antisense assays fall into one or more of the following categories: (i) indirect measurement of protein production, (ii) failure to measure the synthesis of a nontargeted protein as an internal control, and (iii) omission of mismatch and scramble-sequence controls.

Here we demonstrate sequence-specific and gene-specific antisense inhibition by C-5 propyne–substituted phosphorothioate ODNs in a reproducible and controlled assay. This assay uses microinjection and rapid protein analysis to compensate for poor cellular uptake (*1*) and rapid intracellular degradation (*4*) of unmodified ODNs. Plasmids that direct the expression of two target reporter genes, SV40 large T antigen (TAg) and *Escherichia coli* β-galactosidase (β-gal) together with antisense ODNs, were delivered to African Green monkey kidney (CV-1) or rat fibroblast (Rat2) cells by nuclear microinjection, and protein production was monitored by immunofluorescence (*5*). Co-injection of the two plasmids resulted in detectable amounts of each protein in the same cell at 4.5 hours after injection (*5*). A mutant TAg protein with a $Pro^{584} \rightarrow$ Leu substitution was used because it is expressed in greater amounts than the wild-type TAg (*6*) and therefore can be detected more readily. We chose an antisense target sequence located ~150 nucleotides (nt) downstream of the TAg translation initiation codon because this RNA site had been previously targeted with microinjected antisense RNA (*7*). The β-gal expression plasmid provided a control for cytostatic and nonspecific effects of the ODNs.

We studied the structure-activity relation of antisense inhibition by introducing phosphate, sugar, and pyrimidine modifications into ODNs (Fig. 1). These chemical

Gilead Sciences, Inc., 353 Lakeside Drive, Foster City, CA 94404.

*To whom correspondence should be addressed.

modifications enabled us to investigate the binding affinity of the ODNs for the target RNA, their intracellular nuclease stability, and their ability to activate ribonuclease (RNase) H–mediated degradation of the target RNA.

Enhanced binding affinity and nuclease stability of ODNs appeared to be critical for antisense activity, and these requirements were fulfilled by phosphorothioate-modified ODNs that contained the C-5 propyne analogs of uridine and cytidine (*8*). The propyne modification greatly enhances affinity for complementary RNA (cRNA) (*8*, *9*), and the phosphorothioate linkage is resistant to intracellular nuclease degradation (Table 1). The C-5 propyne–substituted ODNs TAg-20d (phosphodiester) and TAg-20e (phosphorothioate) elicited RNase H cleavage of cRNA and completely inhibited TAg expression (Table 1 and Fig. 2A). TAg-20e was approximately 50 times more active than TAg-20d, probably because of the enhanced nuclease resistance conferred by the phosphorothioate modification. Microinjection of 0.5 μM (intracellular concentration) TAg-20e resulted in inhibition of TAg expression for more than 48 hours, whereas microinjection of 25 μM (intracellular concentration) TAg-20d resulted in inhibition for less than 6 hours. Conversely, ODNs that contained thymidine and 5-methyl-2′-deoxycytidine (T-mC) and the phosphodiester (TAg-20a) or phosphorothioate (TAg-20b) linkage (*10*) did not show specific inhibition of TAg expression (Table 1). Nonspecific inhibition of TAg and β-gal expression was observed with all phosphorothioate ODNs at high concentrations (≥20 μM; Table 1).

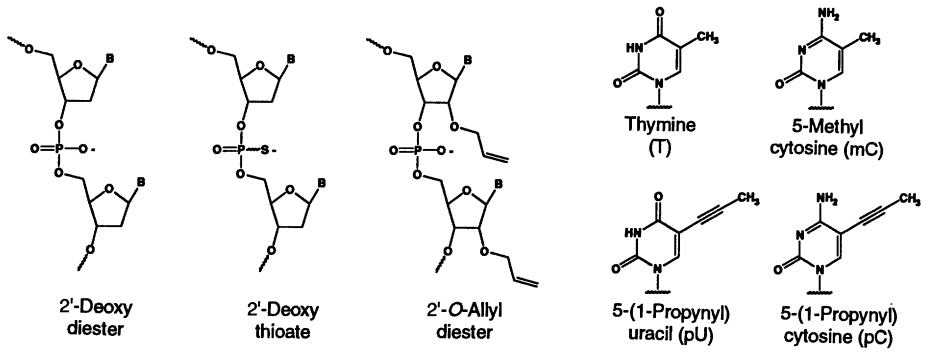

TAg-20	5′ AUU UUC UUC AUU UUU UCU UC 3′	TAg-m1	5′ CUU CAU UAU UUC UUC 3′
TAg-15	5′ CUU CAU UUU UUC UUC 3′	TAg-m4	5′ CUU UCU UUC UUA UUC 3′
TAg-13	5′ CUU CAU UUU UUC U 3′	TAg-m10	5′ UCU UUU CUA UCU CUU 3′
TAg-11	5′ CUU CAU UUU UU 3′		
TAg-9	5′ CUU CAU UUU 3′	β-gal	5′ UUG CCG UUU UCA UCA 3′

Fig. 1. Structures of ODN analogs and ODN sequences. In the structures, B indicates the position of T-mC or pU-pC. In the sequences, U indicates the position of T or pU; C indicates the position of mC or pC; and the underline indicates the position of a mismatch nucleoside. The nucleoside analogs were prepared as described (*8*, *9*). All ODNs were prepared by means of H-phosphonate intermediates (*9*, *20*), purified by PAGE, and analyzed by PAGE and base composition analysis.

Table 1. Biophysical data and biological activity of ODNs in CV-1 cells. Nuclease stability indicates the resistance (+) or susceptibility (−) of ODNs to intracellular nuclease degradation, as measured by a fluorescence assay (*4*). For RNase H assays, the Avr II–Bam HI fragment of pSV40 was cloned into pGEM3Z (Promega), cut with Bst XI, and transcribed with SP6 polymerase (*21*). ODNs (0.05 μM) were added to the [^{32}P]RNA (450 nt, 10^6 cpm/μg, 0.005 μM), and after 10 min the samples were analyzed for cleavage by RNase H [either 5 μg of HeLa extract (Promega) or 1 U of *Escherichia coli* RNase H (Pharmacia)] (*21*); (+) indicates cleavage at the expected target site, and (−) indicates no cleavage. The ODN-RNA T_m values were assessed as described (*9*) and are ±0.5°C. We estimated the IC_{50} values by preparing fivefold dilutions of antisense and control ODNs (*22*) (needle concentration = 0.4 to 400 μM) and scoring for TAg versus β-gal–expressing cells (relative to control injections containing no ODN). The estimated dilution of ODN from needle to cell was 20-fold; there may have been as much as a twofold difference in delivery from cell to cell (*23*). Relative values were taken from a population of 95 to 100 β-gal–expressing cells, and each experiment was repeated in duplicate. Similar results were obtained in Rat2 cells with the exception that TAg-9 selectively inhibited TAg (IC_{50} = 5 μM). NI, no inhibition observed at 20 μM.

ODN	Length (nt)	Modifications	Nuclease stability	RNase H	T_m (°C)	IC_{50} (μM)	
						TAg	β-gal
TAg-20a	20	Diester, T-mC	−	+	54.0	NI	NI
TAg-20b	20	Thioate, T-mC	+	+	40.0	~20	~20
TAg-20c	20	2′-*O*-Allyl, T-mC	+	−	70.0	NI	NI
TAg-20d	20	Diester, pU-pC	−	+	82.5	2.5	NI
TAg-20e	20	Thioate, pU-pC	+	+	76.5	0.05	~20
TAg-20f	20	2′-*O*-Allyl, pU-pC	+	−	89.5	NI	NI
TAg-15	15	Thioate, pU-pC			71.0	0.10	~20
TAg-13	13	Thioate, pU-pC			63.5	0.25	~20
TAg-11	11	Thioate, pU-pC			53.5	1.0	~20
TAg-9	9	Thioate, pU-pC			48.0	>20	>20
TAg-m1	15	Thioate, pU-pC			59.5	0.50	~20
TAg-m4	15	Thioate, pU-pC			43.0	~20	~20
TAg-m10	15	Thioate, pU-pC			~29	~20	~20
β-gal-a	15	Thioate, T-mC			51.0	~20	~20
β-gal-b	15	Thioate, pU-pC			71.5	~20	0.25

RNase H cleavage of nuclear RNA may play a critical role in antisense inhibition. Microinjection of a C-5 propyne phosphorothioate ODN that was complementary to the intron of TAg (*11*) resulted in gene-specific inhibition of TAg [intracellular concentration showing 50% inhibition (IC_{50}) = 0.1 μM], which indicates that cleavage of the RNA occurred within the nucleus. Additionally, the 2′-O-allyl–modified ODNs targeted to the coding region (*9*, *12*), TAg-20c (T-mC) and TAg-20f (pU-pC), did not inhibit TAg expression (Table 1). These ODNs bound to RNA with high affinity [melting temperature (T_m) = 70.0°C and 89.5°C, respectively] and were resistant to nucleases but did not activate RNase H cleavage of the ODN-RNA duplex (Table 1).

The potency of antisense inhibition was dependent on ODN length. We tested C-5 propyne–substituted phosphorothioates in lengths of 20, 15, 13, 11, and 9 nt (Fig. 1) and found that both activity and affinity decreased with decreasing ODN length (Table 1). TAg expression was specifically inhibited by the 11-nt ODN (TAg-11) in both CV-1 and Rat2 cells.

Gene-specific antisense inhibition was also observed with a C-5 propyne–substituted phosphorothioate ODN (15-nt; β-gal-b) that targeted the coding region of β-gal mRNA, ~1900 nt downstream of the β-gal translation initiation codon. The expression of β-gal was specifically inhibited by this ODN (β-gal-b; Fig. 2A) but not by the same phosphorothioate ODN derived from T-mC (β-gal-a; Table 1).

Sequence specificity of antisense inhibition was determined with C-5 propyne

phosphorothioate ODNs (15 nt) containing one, four, and ten mismatches (Fig. 1). The ODN containing one mismatch (TAg-m1) specifically inhibited TAg expression, although the activity and T_m were reduced (Table 1) relative to TAg-15. ODNs that contained four and ten mismatches (TAg-m4 and TAg-m10, respectively) were inactive. Antisense inhibition was dependent on the concentration of ODNs (Fig. 2B). This dose-response effect was typical of all active ODNs.

The activity of the ODNs was dependent on the mode of delivery. TAg-15 did not inhibit TAg expression when incubated in cell media with CV-1, Rat2, or rat brain tumor (smooth muscle–like; BC_3H1) cells at an extracellular concentration of 50 μM (*13*). Likewise, the T-mC phosphodiester and phosphorothioate ODNs (TAg-20a and TAg-20b, respectively) were inactive. In contrast, TAg-15 completely and specifically inhibited TAg expression when microinjected (nuclear; 0.5 μM) into Rat2, BC_3H1, normal human fibroblast (CCD-45Sk), human ovarian carcinoma (SK-OV-3), and human epithelial carcinoma (HeLa) cell lines.

Studies with fluorescent derivatives of TAg-15, TAg-20a, and TAg-20b (Fl-ODNs) showed that when these ODNs were added to the extracellular media (50 μM), they localized to endosomes and lysosomes (Fig. 3A) (*14*). Identical results were obtained with Rat2, BC_3H1, CCD-45Sk, and HeLa cells. However, when these ODNs were microinjected into the cytoplasm, they localized to the nucleus (Fig. 3B). Fluorescence microscopy showed that Fl-ODNs were released from endosomal vesicles by lipofectin, a cell-permeabilization reagent (*15*), and that the Fl-ODNs localized into the nuclei of ~90% of the cells. When TAg-15 was incubated with CV-1 cells in the presence of lipofectin, complete and specific inhibition of TAg expression was observed (0.005 μM media concentration), but under these conditions TAg-m10 did not specifically inhibit TAg expression (*16*). These results suggest that ODNs (uncomplexed) are endocytosed by cells; therefore, the C-5 propyne–substituted phosphorothioate ODNs that were added to the cell media were likely to be trapped in endosomal compartments and rendered inactive. In contrast, the ODN-lipofectin complex allowed the ODN to enter the cells and into the nuclei, and this resulted in gene-specific inhibition.

The C-5 propyne–substituted ODNs were active against two additional RNA target sites. The 5′ untranslated region and the translation initiation codon region of TAg RNA were each targeted with T-mC or C-5 propyne–substituted phosphorothioate ODNs (20 nt). Both C-5 propyne–substituted ODNs selectively inhibited expression of TAg (IC_{50} = 0.1 μM) (*17*). The T-mC phosphorothioate ODN targeted to the 5′ untranslated region showed specific inhibition of TAg, although this occurred over a narrow dose-response range (*17*). This was the only time a T-mC ODN showed sequence-specific antisense activity in our assay.

Antisense inhibition with the potent C-5 propyne–substituted phosphorothioate ODNs was (i) correlated with enhanced binding affinity, enhanced nuclease stability, and RNase H sensitivity, (ii) dependent on length and sequence (mismatch) of the ODN, (iii) gene specific, (iv) independent of RNA target site and cell type, and (v) dependent on the mode of delivery. Our data clearly show that most ODNs that contained T-mC, regardless of the phosphate or sugar modifications tested, were

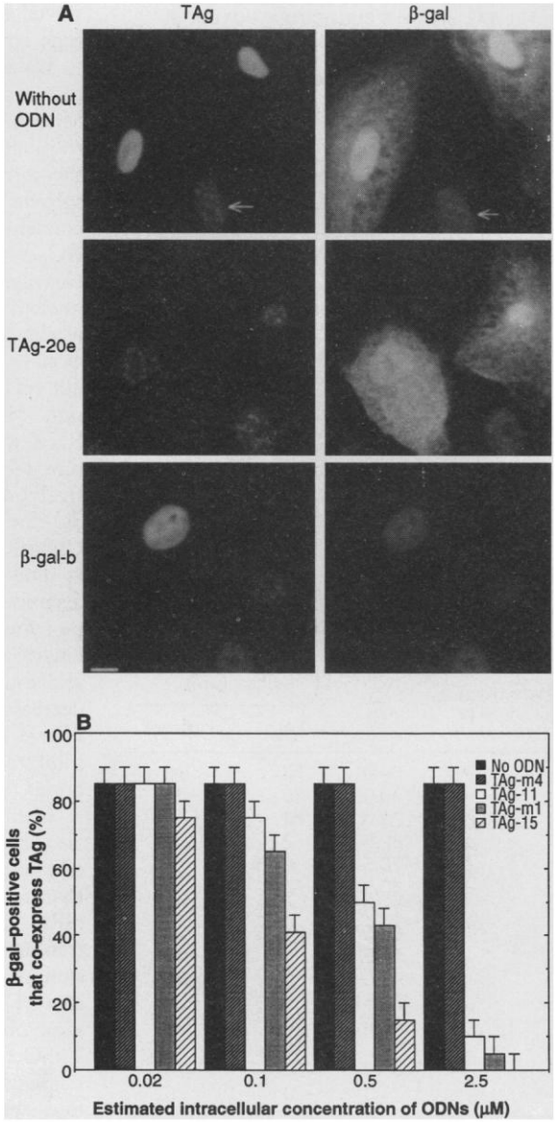

Fig. 2. (**A**) Gene-specific inhibition by C-5 propyne–substituted phosphorothioate ODNs. CV-1 cells were microinjected with or without ODN, together with the TAg and β-gal plasmids, incubated for 4.5 hours, and analyzed (*5*). Upper fields (without ODN) show 2 of 87 cells co-expressing β-gal and TAg (ten additional cells expressed β-gal and no TAg); arrows indicate noninjected cells that displayed nonspecific background staining. Middle fields (TAg-20e, 1 μM) show 2 of the 99 cells expressing β-gal, none of which co-expressed TAg; lower fields (β-gal-b, 1 μM) show 1 of the 95 cells expressing TAg, none of which co-expressed β-gal. These experiments were performed in duplicate. Images were recorded by means of an Axiovert 10 microscope (Zeiss, San Leandro, California) attached to a laser confocal imaging system (Noran Instruments, Middleton, Wisconsin) with a ×63 Plan-apochromat lens. Scale bar equals 10 μm. (**B**) Dose response of inhibition with TAg-15, TAg-11, TAg-m1, and TAg-m4. CV-1 cells were microinjected with no ODN or fivefold dilutions of the indicated ODNs (*5*). Each data point is the mean ± SE of two different experiments, and in all cases 95 ± 5% of injected cells expressed β-gal.

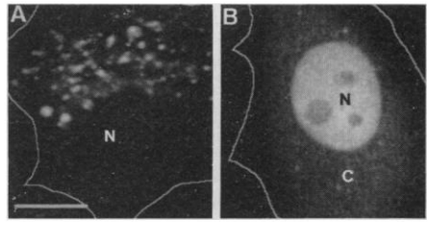

Fig. 3. Permeation of a fluorescent derivative of TAg-15 into CV-1 cells. (**A**) The ODN was incubated for 24 hours in media [50 μM in phenol red minus DMEM (Applied Scientific, South San Francisco, California) plus 10% FBS], washed extensively, and viewed (without fixation) by confocal fluorescence microscopy. Scale bar equals 10 μm. (**B**) The ODN was microinjected into the cytoplasm (0.5 μM intracellular concentration) and viewed (without fixation) 1 hour after injection. N indicates the nucleus, C indicates the cytoplasm, and the three gray areas in the nucleus (B) are the nucleoli.

inactive as antisense inhibitors of gene expression. This inactivity is likely due to the low binding affinity and poor (unaided) cellular uptake of T-mC ODNs. Thus, our data questions many previous results describing antisense-mediated gene inhibition with T and C phosphorothioate and phosphodiester ODNs. The C-5 propyne–substituted phosphorothioates represent a new class of antisense ODNs that may prove to be universal reagents for the inhibition of gene expression.

REFERENCES AND NOTES

1. N. Bischofberger and R. W. Wagner, *Semin. Virol.* **3**, 57 (1992).
2. We have evaluated a variety of ODN analogs in a number of assay systems (*18*) and have found similar biological effects with antisense, mismatch, and scramble-sequence controls.
3. C. A. Stein, J. L. Tonkinson, L. Yakubov, *Pharmacol. Ther.* **52**, 365 (1991).
4. T. L. Fisher, T. Terhorst, X. Cao, R. W. Wagner, *Nucleic Acids Res.*, in press.
5. The TAg plasmid was derived from p5080 (*6*) in which the TAg-containing Kpn I–Bam HI fragment was cloned into pUC19 (Pharmacia, Piscataway, NJ); the β-gal plasmid was pRSVZ. The TAg and β-gal plasmids [needle concentrations of 0.006 and 0.16 μg/μl, respectively, in 80 mM KCl–50 mM Hepes (pH 7.3)] were nuclear microinjected into 100 CV-1 cells. Microinjection was performed on a microscope (Axiovert 10, Zeiss) with a pneumatic controller (PLI-188, Nikon, Garden City, NY) attached to a micromanipulator (MO-302, Narishige U.S.A., Greenvale, NY). The cells were subsequently incubated for 4.5 hours at 37°C, fixed, immunolabeled (*19*), and scored visually by fluorescence microscopy for TAg and β-gal expression. In the absence of co-injected ODNs, 95 ± 5% of the injected cells expressed β-gal and of these, 85 ± 5% co-expressed TAg.
6. L. C. Tack *et al.*, *J. Virol.* **63**, 3962 (1989).
7. M. Graessmann, G. Michaels, B. Berg, A. Graessmann, *Nucleic Acids Res.* **19**, 53 (1991).
8. B. C. Froehler, S. Wadwani, T. J. Terhorst, S. R. Gerrard, *Tetrahedron Lett.* **33**, 5307 (1992).
9. B. C. Froehler, R. J. Jones, X. Cao, T. J. Terhorst, *ibid.* **34**, 1003 (1993).
10. TAg-20a and TAg-20b containing 2′-deoxycytidine produced results identical to those observed with the T-mC ODNs.
11. The 15-nt ODN complementary to the TAg intron was 5′-UUUUCUAUUUUCAUG-3′.
12. A. M. Iribarren *et al.*, *Proc. Natl. Acad. Sci. U.S.A.* **87**, 7747 (1990).
13. Cells were incubated with ODNs for 24 hours, washed, and microinjected (100 cells per experiment) with the TAg and β-gal plasmids (*5*).
14. Cells were incubated with 5′-fluoresceinated TAg-15 (purified by polyacrylamide gel electrophoresis) for 2 hours in the presence of Texas Red–conjugated dextran (average molecular weight = 10,000; Molecular Probes, Eugene, OR; 1 mg/ml), a lysosomal marker. Fluorescence confocal microscopy of the live cells showed that >85% of the lysosomal vesicles contained both fluorophores.
15. M. Y. Chiang *et al.*, *J. Biol. Chem.* **266**, 18162 (1991).
16. TAg-15 or TAg-m10 (0.05 to 0.005 μM) was premixed with lipofectin (Gibco BRL, Gaithersburg, MD; 10 μM) and added to CV-1 cells in Opti-modified Eagle's medium (Gibco BRL). After 4 hours, the cells were washed and incubated for an additional 16 hours in Dulbecco's modified Eagle's medium plus 10% fetal bovine serum (FBS). One hundred cells were microinjected with the TAg and β-gal plasmids and analyzed (*5*).
17. The 20-nt ODN sequence used to target the 5′-untranslated region was 5′-GCCUCCUCACUACUUCUGGA-3′ and that used to target the translation initiation codon region was 5′-CAUCUUUGCAAAGCUUUUUG-3′. The T-mC phosphorothioate ODNs were each inactive at 1 μM, and each inhibited TAg and β-gal expression at 20 μM (*5*). The T-mC ODN targeted to the 5′-untranslated region specifically inhibited TAg expression at 5 μM, whereas the ODN targeted to the initiation codon partially inhibited both TAg and β-gal expression at 5 μM.
18. G. Anfossi, A. M. Gewirtz, B. Calabretta, *Proc. Natl. Acad. Sci. U.S.A.* **86**, 3379 (1989); A. Rosolen, L. Whitesell, N. Ikegaki, R. H. Kennett, L. Neckers, *Cancer Res.* **50**, 6316 (1990); M. Simons and R. D. Rosenberg, *Circ. Res.* **70**, 835 (1992); K. G. Draper, D. J. Ecker, C. K. Mirabelli, S. T. Crooke, International Patent Application WO 91/12811 (1991).
19. J. C. Hanvey *et al.*, *Science* **258**, 1481 (1992).
20. B. C. Froehler, in *Protocols for Oligonucleotides and Analogs: Synthesis and Properties*, S. Agrawal, Ed. (Humana, Totowa, NJ, 1993), pp. 63–80.
21. S. Young and R. W. Wagner, *Nucleic Acids Res.* **19**, 2463 (1991).
22. The control sequence was 5′-UUAUUAUCUUCUUCUUUUCU-3′ and contained 11 mismatches. Antisense ODNs were directly compared with control ODNs at concentrations tenfold more than the IC_{50} of the antisense ODN, and the control ODNs showed no activity.
23. M. Graessmann and A. Graessmann, *Methods Enzymol.* **101**, 482 (1983).

24. We thank T. Fisher, T. Terhorst, and S. Wadwani for technical assistance; J. Pipas for the p5080 plasmid; and J. Milligan for valuable discussions. All other cells and plasmids (pSV40 and pRSVZ) were purchased from the American Type Culture Collection. This work was supported in part by a contract from the Defense Advanced Research Projects Agency.

9 December 1992; accepted 23 March 1993

Relation of Phenotype Evolution of HIV-1 to Envelope V2 Configuration

Martijn Groenink,* Ron A. M. Fouchier, Silvia Broersen, Catriona H. Baker, Maarten Koot, Angélique B. van't Wout, Han G. Huisman, Frank Miedema, Matthijs Tersmette, Hanneke Schuitemaker

Biological variability of human immunodeficiency virus type–1 (HIV-1) is involved in the pathogenesis of acquired immunodeficiency syndrome (AIDS). Syncytium-inducing (SI) HIV-1 variants emerge in 50 percent of infected individuals during infection, preceding accelerated CD4+ T cell loss and rapid progression to AIDS. The V1 to V2 and V3 region of the viral envelope glycoprotein gp120 contained the major determinants of SI capacity. The configuration of a hypervariable locus in the V2 domain appeared to be predictive for non-SI to SI phenotype conversion. Early prediction of HIV-1 phenotype evolution may be useful for clinical monitoring and treatment of asymptomatic infection.

There is increasing evidence for a role of biological variability of HIV-1 in the pathogenesis of AIDS (*1–4*). In the asymptomatic phase of infection, predominantly non–syncytium-inducing (NSI), monocytotropic HIV-1 variants can be detected (*5*). In about 50% of the cases SI HIV-1 variants emerge in the course of infection, preceding rapid CD4+ T cell depletion and progression to AIDS (*6, 7*). Moreover, we recently obtained evidence that there is a major beneficial effect of zidovudine treatment in asymptomatic individuals who harbor NSI variants and do not develop SI variants during treatment (*8*). These findings prompted us to try to identify determinants within the viral genome that may be predictive for the future emergence of SI variants in an individual.

Previously we generated NSI and SI molecular HIV-1 clones from a single individual at the time of NSI to SI switch (*9*). In agreement with others, we have shown that the gene *env* is the major determinant responsible for differences in biological properties (*10–16*). Sequence analysis revealed that variation in the NH_2-terminal part of gp120, the C1 up to V4 region, segregated with the capacity to induce syncytia in peripheral blood mononuclear cells (PBMC) (*15*). To investigate if differences in SI capacity were determined by the C1 to V4 region, recombinant viruses were constructed in which sequences within this region were exchanged between an NSI and SI clone (Fig. 1).

Reciprocal exchanges between the NSI and SI clone of the V1 up to C2 region (Fig. 1, A and E), the COOH terminus of V1 ($V1_{C\text{-}term}$) up to the V2 region (Fig. 1, B and F), or the V3 up to V4 region (Fig. 1, C and G) resulted in recombinant viruses that induced occasional, small syncytia in PBMC. Primary SI isolates are characterized by their capacity to replicate and induce syncytia in the MT-2 T cell line (*17*). All recombinant viruses described above

Department of Clinical Viro-Immunology, Central Laboratory of the Netherlands Red Cross Blood Transfusion Service and Laboratory for Experimental and Clinical Immunology of the University of Amsterdam, Plesmanlaan 125, 1066 CX Amsterdam, The Netherlands.

*To whom correspondence should be addressed.